Asymmetry reversal of thermomagnetic avalanches in Pb films with a ratchet pinning potential

M. Menghini,[1] J. Van de Vondel,[1] D. G. Gheorghe,[2] R. J. Wijngaarden,[2] and V. V. Moshchalkov[1]
[1]*Nanoscale Superconductivity and Magnetism & Pulsed Fields Group, INPAC-Institute for Nanoscale Physics and Chemistry, Katholieke Universiteit Leuven, Celestijnenlaan 200D, Leuven B-3001, Belgium*
[2]*Department of Physics and Astronomy, Faculty of Sciences, Vrije Universiteit, De Boelelaan 1081, 1081HV Amsterdam, The Netherlands*
(Received 12 October 2007; published 19 November 2007)

We combine transport measurements and magneto-optical imaging in order to study vortex motion in Pb samples with a square lattice of asymmetric pinning potentials formed by two antidots of different sizes. Near the boundary with the normal phase, a vortex ratchet effect is detected when an ac-current is applied. As previously observed in similar systems, inversion of vortex rectification direction occurs as the magnetic field is changed. Further inside the superconducting phase, anisotropic flux penetration patterns are formed. An inversion of anisotropy is observed as the temperature is lowered. This effect can be understood in terms of a thermomagnetic avalanche model.

DOI: 10.1103/PhysRevB.76.184515 PACS number(s): 74.78.Db, 74.25.Qt, 74.78.Na, 74.25.−q

I. INTRODUCTION

Vortex motion in superconductors in the presence of periodic pinning arrays has been studied for long time both from the experimental and theoretical point of view.[1] Lately, the attention has been turned to vortex dynamics in the presence of periodic pinning potentials formed by asymmetric pinning sites.[2–6] In this case, rectification of vortex motion can be induced by an unbiased force, which is a *ratchet effect*. Interestingly, reversal of motion direction occurs as the magnetic field, which defines the number of vortices, is changed. In particular, several reversal of motion direction, close to the superconductor-normal phase boundary, have been observed in Al samples with a nanoengineered square array of big and small antidots one next to the other.[7] Molecular dynamics simulations of strongly interacting particles in a one-dimensional ratchet potential show[7] a controlled reversal motion as the number of particles changes from odd to even in agreement with experimental results. The results were explained considering that the effective energy of particles in the potential wells follows a sort of brick-wall tiling pattern. Thus, as the number of particles increases, the new particles sit alternatively in the deep and shallow well. In this case, the particle drift direction depends on the number of particles per unit cell.

Rectification of vortex motion was observed in real space by means of Lorentz microscopy[8] and scanning Hall probe imaging.[9] In the first case, the experiments were performed in Nb films patterned by focused ion beam irradiation.[8] The asymmetric potential was formed by asymmetric channels that acted as "funnels" for vortex motion and the unbiased force was generated by oscillating the applied magnetic field. In the last case, the experiments show[9] a net dc vortex motion in $Bi_2Sr_2CaCu_2O_{8+\delta}$ crystals when applying a time asymmetric drive.

On the other hand, it is well known that flux penetration patterns in superconductors can be affected by the presence of strong pinning sites such as periodic arrays of antidots.[10–14] Vortex channeling along the principal direction of the lattice vector of the pin array has been observed.[10,13] Anisotropic flux penetration occurs when vortices interact with either anisotropic arrays of pinning sites[13] or arrays of anisotropic pinning sites.[14] In particular, the effects of the pinning potential are more pronounced in the region of the magnetic field (H)–temperature (T) phase diagram where vortices enter the sample very abruptly in the form of dendritic avalanches.[11,12] It has been shown that this dendritic instability is a result of the coupling between magnetic flux diffusion and local heating induced by vortex motion.[15,16] In the case of a sample with a square lattice of rectangular antidots, vortices penetrate forming dendrites elongated parallel to the long side of the rectangles with almost no side branches.[14]

Anisotropic flux penetration can also be induced in isotropic superconducting samples grown on top of an anisotropic substrate.[17,18] For example, in Ref. 18, MgB_2 films were grown on substrates that have parallel steps. In this way, different critical currents for vortex motion parallel and perpendicular to the steps are induced. Interestingly, at temperatures close to 10 K, it is seen[18] that vortices move further into the sample at the edges with the largest critical current. This means that the flux penetration is also larger in the direction perpendicular to the largest critical current, contrary to what one would expect in superconductors obeying the Bean model. This unexpected anisotropy is observed to occur in the dendritic penetration regime. In this case, the anisotropy of the flux pattern is not only inverse but also much larger than the one expected from the anisotropy of the critical current. At higher temperatures, where a Bean-like profile is formed, this inverse flux penetration is no longer observed. At lower temperatures, the vortex penetration pattern is isotropic. These results were explained by a thermomagnetic model of the dendritic instability.[16,19]

In this paper, we study vortex motion in superconducting Pb samples with arrays of antidots forming a periodic lattice with *broken inversion symmetry*. The transport properties of the sample were investigated using a Quantum Design cryostat with conventional electronics. Using magneto-optical imaging, we were able to follow the formation of flux penetration patterns in the sample at different temperatures. Figure 1 shows an atomic force microscopy (AFM) picture of the sample and a schematic drawing of the configuration of

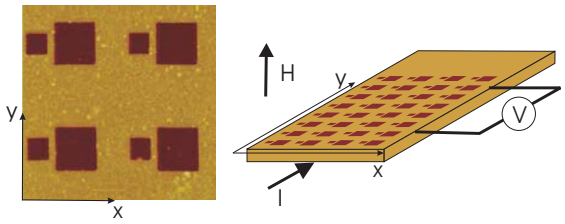

FIG. 1. (Color online) AFM image of the sample and schematics of the current and voltage contact configuration. The lattice parameter of the array is 3 μm. The big (small) square antidots have a lateral size of 1200 nm (600 nm).

current and voltage contacts used in the experiments. By means of e-beam lithography, a square array of big (1200×1200 nm^2) and small (600×600 nm^2) holes (antidots) was engineered in a trilayer Ge(10 nm)/Pb(75 nm)/Ge(100 nm). The array of dots forms a square lattice with period $a = 3$ μm. This period gives a matching field $\mu_0 H_1 = 0.23$ mT. Part of the sample was not patterned in order to have a reference plain region. The sample has a rectangular shape with a width of 600 μm. In the transport measurements, the current was applied along the y direction (see Fig. 1) and the voltage was measured longitudinally. The magnetic field was applied perpendicular to the surface of the sample. The magneto-optical technique allows the observation of the distribution of magnetic induction B on the surface of the sample. In the images that we will show below, the brighter regions correspond to higher B. A detailed description of the sample fabrication and the magneto-optical technique can be found in Refs. 20 and 21, respectively.

II. RESULTS AND DISCUSSION

We first investigate the rectification of vortex motion induced by an ac-current. Figure 2(a) shows dc-voltage curves as a function of reduced magnetic field, H/H_1, for different reduced temperatures, $t = T/T_c$ ($T_c = 7.21$ K). The current has an amplitude of $I_{ac} = 0.5$ mA and a frequency of 1.1 kHz. At $t = 0.998$, vortex rectification is detected around $H/H_1 = \pm 1$ and $H/H_1 = \pm 2.5$. The negative sign of the dc-voltage at $H/H_1 = +1$ corresponds to vortices moving in the negative x direction (see Fig. 1). As previously shown,[6] this is the *easy* direction of vortex motion for the asymmetric pinning potential generated by the array of small and big antidots. The change in sign in V_{dc} when going from first matching field to $H/H_1 = \pm 2.5$ indicates that the vortex motion direction is reversed. As the temperature is lowered, V_{dc} shows several sign changes. The change in sign of the vortex motion direction is also evident in Fig. 2(b) where a contour plot of V_{dc} as a function of H/H_1 and I_{ac} at $t = 0.99$ is shown. From the experimental results, it is clear that the sign of V_{dc} changes when H/H_1 goes from 1 to 2. However, no sign reversal is observed from $H/H_1 = 2$ to $H/H_1 = 3$. At $H/H_1 = 4$, the vortices are rectified in the same direction as at $H/H_1 = 2$. The reversal of vortex motion in superconductors with asymmetric periodic pinning potentials was previously explained by molecular dynamics simulations that consider the vortices as

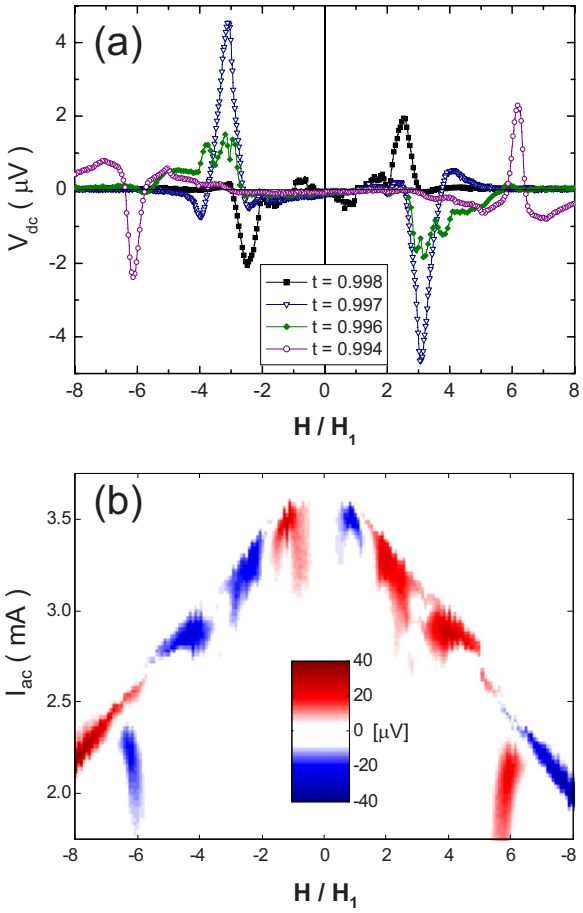

FIG. 2. (Color online) (a) dc-voltage curves as a function of reduced field H/H_1 for different reduced temperatures t. The applied ac-current has a magnitude of $I_{ac} = 0.5$ mA. (b) Contour color plot of dc-voltage as a function of H/H_1 and I_{ac} at $t = 0.99$. In both cases, the frequency of the ac-current is 1.1 kHz.

a system of highly interacting particles.[7] The previous results show clear evidence that the pinning potential produced by the array of asymmetric antidots induces a vortex ratchet effect in Pb samples at temperatures close to the transition to the normal state.

It is interesting to see now the effects of the asymmetric pinning potential on the flux penetration process. In this case, as the vortices enter the sample from the edge, a quite inhomogeneous vortex distribution is expected. In Fig. 3, sequences of flux penetration patterns obtained by magneto-optical imaging at $t = 0.93$ [(a)–(c)] and $t = 0.28$ [(d)–(f)] are shown. The images were taken increasing the applied field after *zero field cooling* (ZFC) the sample down to the desired temperature. The corresponding values of $\mu_0 H$ are indicated below each picture. The upper parts of the images (above dotted line) correspond to the plain region of the sample. The vertical borders of the images correspond to the edges of the sample. In Fig. 3(a), a schematic drawing indicates the orientation of the big and small antidots with respect to the edge of the sample. As expected, in the plain regions, the flux penetrates symmetrically from the left and right edges. However, in the patterned region and at $t = 0.93$, magnetic flux

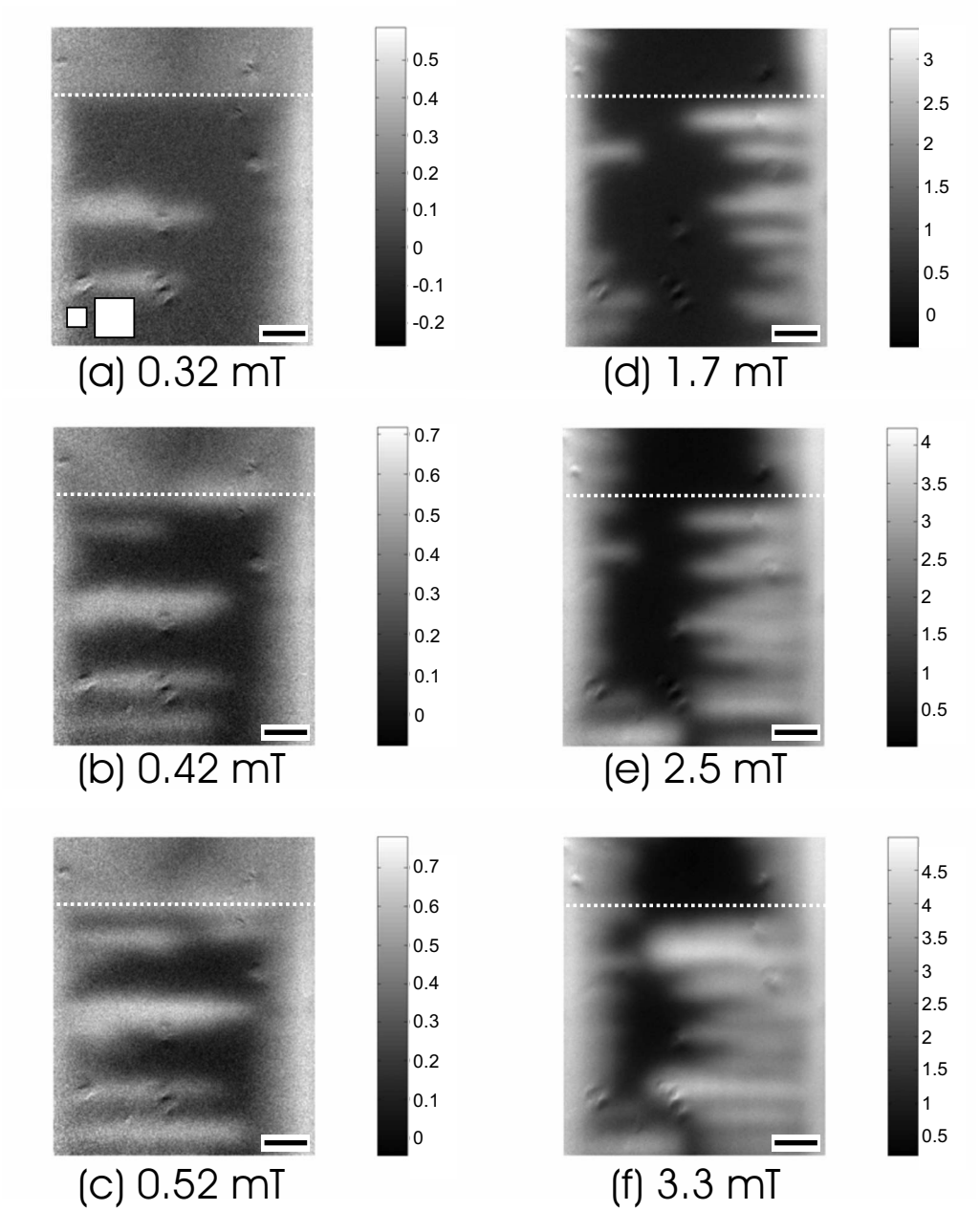

FIG. 3. Sequence of flux penetration patterns at [(a)–(c)] $t=0.93$ and [(d)–(f)] $t=0.28$ increasing H after ZFC the sample. The corresponding applied fields are indicated below each image. The dotted lines indicate the border between patterned (lower part) and nonpatterned (upper part) regions. The scale bars correspond to 100 μm and the color bars indicate the values of B in mT.

penetrates the sample mainly from the left edge. Vortices burst into the sample in the form of dendrites elongated in the direction perpendicular to the sample edge. As previously observed[11,12] in samples with periodic and symmetric arrays of antidots, there is clear evidence of channeling of vortices along the lattice vector of the antidot lattice. In our sample, the dentritic penetration region is extended up to higher temperatures than previously reported results in Pb films with an array of symmetric antidots.[12] It has been established that the presence of a periodic array of antidots and the consequent increase in critical current produce an enlargement of the region in the phase diagram where the dendritic instability occurs as compared with unpatterned samples.[12] In the present case, the larger size of the holes (1200 nm) as compared with previous cases (500 or 800 nm, see Refs. 12, 22, and 23) induces a higher critical current[24] and consequently favors dendritic penetration at higher temperatures. Interestingly, at $t=0.28$, vortex entry occurs preferentially from the *opposite edge* of the sample (the right hand one) as compared with $t=0.93$. As before, the flux front profile is very irregular due to the dendritic character of flux penetration. At the intermediate temperature of $t=0.69$, more symmetric flux penetration and smoother flux fronts are observed (not shown). Although for $t>0.97$ the contrast of the images is quite low, it is possible to observe that, in this range of temperatures, the flux fronts are also symmetric.

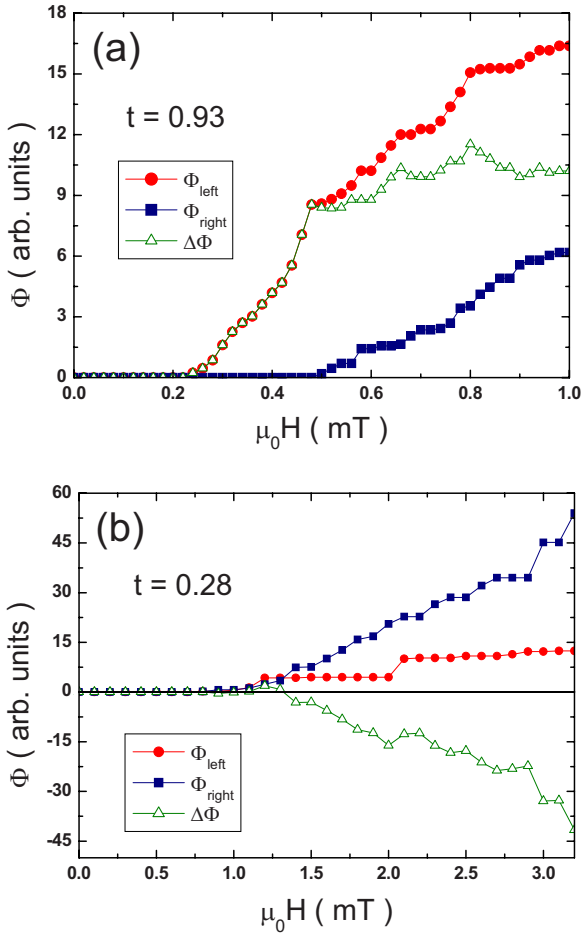

FIG. 4. (Color online) Magnetic flux Φ that enters the sample from left and right edges of the sample as a function of applied field. (a) $t=0.93$ and (b) $t=0.28$.

In order to characterize the asymmetry of flux penetration as a function of temperature, we have calculated separately the total flux that penetrates from the left (Φ_{left}) and the right (Φ_{right}) edges of the sample as a function of the applied field H. The calculation is made as follows. First, images taken at two consecutive values of H are subtracted. Then, the area occupied by each dendrite, A_d, is identified and the flux associated with each dendrite is calculated as $\Phi_d=B_dA_d$. Dendrites coming from the left edge are separated from the ones coming from the right. The values for Φ_{left} and Φ_{right} are obtained summing up all the flux corresponding to the dendrites entering from the left and right, respectively, see Fig. 4. At $t=0.93$, the difference between the flux that enters from the left and the flux that enters from the right is evident, see Fig. 4(a). It is also clear that vortices start to enter the left side at $\mu_0H\sim0.2$ mT, while H has to be increased up to approximately 0.5 mT such that vortices penetrate from the right. Thus, the difference in flux $\Delta\Phi=\Phi_{left}-\Phi_{right}$ increases rapidly up to $\mu_0H\sim0.5$ mT. At higher fields, the difference remains more or less constant. At low temperature, $t=0.28$, vortices penetrate almost simultaneously from the left and from the right edges. However, the rate of flux penetration is much faster from the right edge, giving rise to an asymmetry in flux penetration, see Fig. 4(b). The sign of $\Delta\Phi$ is reversed

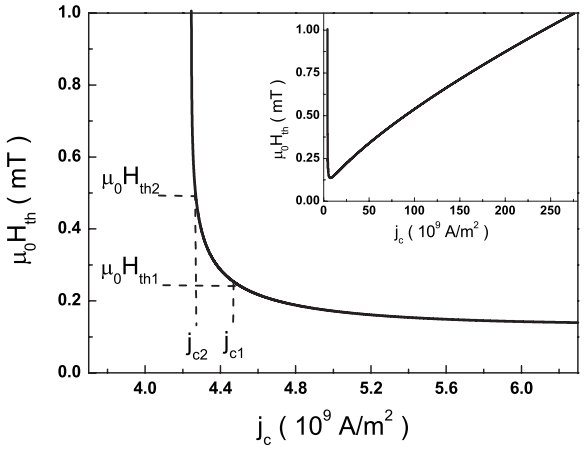

FIG. 5. Threshold field for the dendritic instability as a function of critical current density. The inset shows the behavior of H_{th} over a wider range in j_c.

as compared to $t=0.93$, accordingly with the reversal of flux penetration direction, see Fig. 3.

Considering the orientation of the antidot lattice with respect to the sample edges [see Fig. 3(a)], the *easy direction* for vortex motion would be from right to left. Taking this into account, the stronger flux penetration from the left edge at high temperatures seems to be counterintuitive. Since this behavior occurs in a wide range of fields, an explanation based on the brick-wall tiling pattern will not be appropriate. On the other hand, it was previously observed[18] in other superconductors that in the regime of dendritic avalanches, there is a range of temperatures where an anisotropy of critical current can induce an inverse anisotropy in flux penetration. As we mentioned in the Introduction, this unexpected anisotropy was explained[18] in terms of a thermomagnetic model for the dendritic instabilities in thin films. Within this model, it is possible to calculate the threshold field for the first dendrite to penetrate the sample as a function of critical current density, $H_{th}(j_c)$. We have calculated $H_{th}(j_c)$ for our sample using Eqs. (1) and (2) from Ref. 18 and found the nonmonotonic relation shown in Fig. 5. At low j_c, we observed that a particular order of critical current density, for example, $j_{c1}>j_{c2}$, corresponds to an inverted order of the threshold field $H_{th1}<H_{th2}$. In a sample with anisotropic j_c, this inversion will cause that dendrites will be formed at lower fields in the region with larger critical current. This is exactly what we observed in our Pb film at $t=0.93$. The values of H_{th1} and H_{th2} indicated in Fig. 5 correspond to the experimental values of magnetic field for dendrite formation on the left and right edges at $t=0.93$, respectively. A difference in threshold field of a factor of 2 can be induced by a difference in j_c of only 4%. Moreover, and also in agreement with the predictions of the thermomagnetic model,[18] this reversed anisotropy is observed close to the threshold temperature above which the dendritic instability disappears (in the present case, it is observed that at $t=0.97$, flux penetration is smooth).

The model also anticipates that, for high enough anisotropy, at low temperatures, the opposite anisotropy should occur, that is, vortices will move easily in the region of low

critical current. This is clearly seen in the inset of Fig. 5 where an upward slope of H_{th} vs j_c at high values of j_c (equivalent to low T) is observed. In our samples, we do observe this inversion in flux penetration direction at low temperatures, see Figs. 3(d)–3(f). However, our results also show that the threshold field for dendritic penetration is almost the same, at least within our resolution, from both edges [Fig. 4(b)]. It is interesting to note that at high temperature (j_c between j_{c2} and j_{c1} in the main panel of Fig. 5), the slope of the curve $d(\mu_0 H_{th})/d(j_c)$ is of the order of 1 mT/(10^9 A/m^2), while at low temperature (for example, at $j_c = 200\ 10^9$ A/m^2, see inset of Fig. 5), the slope is $d(\mu_0 H_{th})/d(j_c) = 0.003$ mT/(10^9 A/m^2). Hence, the same difference $j_{c2} - j_{c1}$ gives a much smaller difference $H_{th2} - H_{th1}$ at high j_c than at lower values. Since the value of j_c is large at low temperature, the ratio H_{th2}/H_{th1} becomes very close to 1 in that limit, as is indeed experimentally observed [Fig. 4(b)]. Although the difference in the onset for avalanches is very small, the asymmetry of flux penetration can be quite large [see Figs. 3(d)–3(f)]. This could be caused by a suppression of avalanches from the left side induced by the disturbance of current flow produced by the avalanches coming from the right. A similar behavior was observed in the MgB_2 samples studied in Ref. 18.

III. CONCLUSIONS

The combination of transport measurements and magneto-optical imaging has allowed us to detect two types of inversion of vortex motion in Pb samples with an array of asymmetric pinning sites. Near the boundary with the normal phase, rectification of vortex motion is induced by an ac-drive. Multiple reversal of the drift direction is observed as the magnetic field is increased. As previously discussed,[7] this inversion can be related with the change in effective energy of interacting particles in the presence of asymmetric pinning potential. On the other hand, visualization of flux penetration shows that deep inside the superconducting region, there is a preferential direction for vortex entry. At high temperatures, vortices move preferentially in the *hard* direction of motion, while at low temperatures, the situation is reversed. This interesting behavior is consistent with the prediction of a thermomagnetic model of the dendritic instability in thin superconducting films.[16,18,19] The model predicts a nonmonotonic behavior of the threshold field for the formation of the first dendrite with critical current density. In agreement with the results of this model, we observed that at high temperatures, the first dendritic avalanches occur in the high critical current region (leading to the largest flux penetration in the high j_c region), while at low temperatures, the dendritic avalanches lead to the largest flux penetration in the low critical current region.

ACKNOWLEDGMENTS

This work was supported by the Belgian Interuniversity Attraction Poles IAP, the Research Fund K.U.Leuven GOA/2004/02, the Flemish FWO, the ESF "Nanoscience and Engineering in Superconductivity (NES)" programmes, and also by FOM (Stichting voor Fundamenteel Onderzoek der Materie) which is financially supported by NWO (Nederlandse Organisatie voor Wetenschappenlijk Onderzoek). J.V.d.V. is grateful for the support from the FWO-Vlaanderen.

[1] A. T. Fiory, A. F. Hebard, and S. Somekh, Appl. Phys. Lett. **32**, 73 (1978); M. Baert, V. V. Metlushko, R. Jonckheere, V. V. Moshchalkov, and Y. Bruynseraede, Phys. Rev. Lett. **74**, 3269 (1995); C. Reichhardt, J. Groth, C. J. Olson, S. B. Field, and F. Nori, Phys. Rev. B **54**, 16108 (1996); V. V. Moshchalkov, V. Bruyndoncx, L. Van Look, J. Bekaert, M. Van Bael, and Y. Bruynseraede, in *Quantum Mesoscopic Phenomena and Mesoscopic Devices in Microelectronics*, edited by I. O. Kulik and R. Ellialtioglu (Kluwer Academic, Dordrecht, 2000), pp. 329–345 and references therein; C. G. R. Berdiyorov, M. V. Milosevic, and F. M. Peeters, Phys. Rev. B **74**, 174512 (2006).

[2] C. S. Lee, B. Janko, I. Derenyi, and A. L. Barabasi, Nature (London) **400**, 337 (1999).

[3] J. F. Wambaugh, C. Reichhardt, C. J. Olson, F. Marchesoni, and F. Nori, Phys. Rev. Lett. **83**, 5106 (1999).

[4] S. Savelév, F. Marchesoni, and F. Nori, Phys. Rev. Lett. **91**, 010601 (2003).

[5] J. E. Villegas, S. Savelév, F. Nori, E. M. Gonzalez, J. V. Anguita, R. Garcia, and J. L. Vicent, Science **302**, 1188 (2003).

[6] J. Van de Vondel, C. C. de Souza Silva, B. Y. Zhu, M. Morelle, and V. V. Moshchalkov, Phys. Rev. Lett. **94**, 057003 (2005).

[7] C. C. de Souza Silva, J. van de Vondel, M. Morelle, and V. V. Moshchalkov, Nature (London) **440**, 651 (2006).

[8] Y. Togawa, K. Harada, T. Akashi, H. Kasai, T. Matsuda, F. Nori, A. Maeda, and A. Tonomura, Phys. Rev. Lett. **95**, 087002 (2005).

[9] D. Cole, S. Bending, S. Savelév, A. Grigorenko, T. Tamegai, and F. Nori, Nat. Mater. **5**, 305 (2006).

[10] R. Surdeanu, R. J. Wijngaarden, R. Griessen, J. Einfeld, and R. Woordenweber, Europhys. Lett. **54**, 682 (2001).

[11] S. Kolesnik, V. Vlasko-Vlasov, U. Welp, G. W. Crabtree, T. Piotrowski, J. Wrobel, A. Klimov, P. Przyslupski, T. Skoskiewicz, and B. Dabrowski, Physica C **341**, 1093 (2000).

[12] M. Menghini, R. J. Wijngaarden, A. V. Silhanek, S. Raedts, and V. V. Moshchalkov, Phys. Rev. B **71**, 104506 (2005).

[13] M. S. Welling, R. J. Wijngaarden, C. M. Aegerter, R. Wordenweber, and P. Lahl, Physica C **404**, 410 (2004).

[14] D. G. Gheorghe, M. Menghini, R. J. Wijngaarden, S. Raedts, A. V. Silhanek, and V. V. Moshchalkov, Physica C **437**, 69 (2006).

[15] E. Altshuler and T. H. Johansen, Rev. Mod. Phys. **76**, 471 (2004).

[16] I. S. Aranson, A. Gurevich, M. S. Welling, R. J. Wijngaarden, V. K. Vlasko-Vlasov, V. M. Vinokur, and U. Welp, Phys. Rev. Lett. **94**, 037002 (2005).

[17] M. Djupmyr, G. Cristiani, H. U. Habermeier, and J. Albrecht, Phys. Rev. B **72**, 220507(R) (2005).

[18] J. Albrecht, A. T. Matveev, J. Strempfer, H. U. Habermeier, D. V.

Shantsev, Y. M. Galperin, and T. H. Johansen, Phys. Rev. Lett. **98**, 117001 (2007).
[19] D. V. Denisov, A. L. Rakhmanov, D. V. Shantsev, Y. M. Galperin, and T. H. Johansen, Phys. Rev. B **73**, 014512 (2006).
[20] S. Raedts, A. V. Silhanek, M. J. Van Bael, and V. V. Moshchalkov, Phys. Rev. B **70**, 024509 (2004).
[21] R. J. Wijngaarden, K. Heeck, M. Welling, R. Limburg, M. Pannetier, K. van Zetten, V. L. G. Roorda, and A. R. Voorwinden, Rev. Sci. Instrum. **72**, 2661 (2001).
[22] S. Hébert, L. Van Look, L. Weckhuysen, and V. V. Moshchalkov, Phys. Rev. B **67**, 224510 (2003).
[23] A. V. Silhanek, S. Raedts, and V. V. Moshchalkov, Phys. Rev. B **70**, 144504 (2004).
[24] V. V. Moshchalkov, M. Baert, V. V. Metlushko, E. Rosseel, M. J. Van Bael, K. Temst, Y. Bruynseraede, and R. Jonckheere, Phys. Rev. B **57**, 3615 (1998).